Atypically depleted upper mantle component revealed by Hf isotopes at Lucky Strike segment

Cédric Hamelin, Antoine Bézos, Laure Dosso, Javier Escartin, Mathilde Cannat, Catherine Mevel

Chemical Geology
March 2013, Volume 341, Pages 128–139
http://dx.doi.org/10.1016/j.chemgeo.2013.01.013

Atypically depleted upper mantle component revealed by Hf isotopes at Lucky Strike segment

Cédric Hamelin[a,*], Antoine Bezos[b], Laure Dosso[c], Javier Escartin[d], Mathilde Cannat[d], Catherine Mevel[d]

[a] Centre for Geobiology, University of Bergen, Allegaten 41N-5007 Bergen, Norway
[b] Laboratoire de Planetologie et de Géodynamique, 2 rue de la Houssiniere, 44322 Nantes BP 92208 Cedex 3, France
[c] Centre National de la Recherche Scientifique, UMR 6538, IFREMER, BP70, 29280 Plouzané, France
[d] Institut de Physique du Globe de Paris, Marines Geosciences, 1 rue Jussieu, 75252 Paris CEDEX 05, France

*: Corresponding author : Cédric Hamelin, email address : ced.hamelin@gmail.com

Abstract:

The Earth's upper mantle is commonly depicted as a “marble cake” assemblage of a refractory component mingled with varying amounts of geochemically diverse enriched components. This depleted component controls the major element composition of Mid-Oceanic Ridge Basalts (MORBs). It has long been considered a fairly uniform reservoir, depleted by early melting and well homogenized by subsequent convective stirring. We present new Hf, Nd, Pb and Sr isotopes and trace element data for basalts from the center of the Lucky Strike segment of the Mid-Atlantic Ridge (MAR). Despite the limited size of our sampling area (1.6 km along-axis by 5 km across), these data show a large range of isotopic compositions (similar to that of the whole MAR). It has recently been shown that part of the reason for not observing more segments with correlated Hf–Nd isotope systematics may be the lack of fine-scale sampling. Our data confirm this idea and show strong correlations between all isotope ratios. The systematics of Hf–Nd isotopes in Lucky Strike basalts define an atypical correlation, distinct from the global mantle array, with an anomalously high εHf for a given εNd. We illustrate that this atypical trend is the signature of an ancient refractory mantle rather than the product of kinetic processes during the melting event. The existence of this mantle component at Lucky Strike allows us to discuss the structure of the upper mantle around the Azores.

Highlights

► High spatial resolution sampling of MAR segment shows small scale mantle heterogeneity. ► Samples define an atypical Hf–Nd isotope correlation, distinct from the mantle array. ► Upper mantle near the Azores hotspot contains different refractory components.

Keywords: Oceanic basalts ; Mid-Atlantic Ridge ; Lucky Strike ; Mantle heterogeneity ; Hf isotopes

1. Introduction

It is now well established that the upper mantle is heterogeneous (Hofmann et al., 2003). This geochemical heterogeneity is evidenced by the composition of basalts which erupted along mid-oceanic ridges, which reveals the existence of broad mantle isotopic domains (e.g., the DUPAL anomaly (Dupré and Allègre, 1983)). Each mantle domain is characterized by its intrinsic lithological and geochemical heterogeneity, suggesting different convective histories (Hamelin et al., 2011; Hanan et al., 2004; Meyzen et al., 2007; Vlastelic et al., 1999). At a local scale, basalt geochemical variations are interpreted toto resultfrom partial melting of a marble-cake upper mantle (Allègre et al., 1984; Morgan and Morgan, 1999; Stracke et al., 2005). This geochemical heterogeneity of ridge basalts has been explained by the addition of various amounts of the FOZO component (Hanan and Graham, 1996; Hart et al., 1992; Stracke et al., 2005) to a uniformly depleted source (Depleted MORB Mantle, DMM). This second asthenospheric component is commonly inferred to have been depleted by previous melting events but subsequently homogenized by convective stirring (Zindler and Hart, 1986). However, recent studies of abyssal peridotites have revealed thatdistinct ancient depletion signals may still be identified in refractory mantle domains (Harvey et al., 2006; Liu et al., 2008; Salters and Dick, 2002; Seyler et al., 2003; Stracke et al., 2011). This observation adds a new level of complexityto the interpretation of MORB data and emphasizes the heterogeneous nature of the depleted mantle.

Lu–Hf and Sm–Nd isotope systems have proven to be useful in tracking the signatures of ancient mantle depletion (e.g., Andres et al., 2004; Graham et al., 2006; Salters et al.; Stracke et al., 2011). Their parent/daughter ratios are higher in the residue than in the melt, thus developing a radiogenic signature in time. The similar behavior of these two radiogenic isotope systems during mantle melting results in strongly correlated $^{177}Hf/^{176}Hf$ –$^{143}Nd/^{144}Nd$ in oceanic basalts, the so-called

49 "mantle array" (Patchett and Tatsumoto, 1980). However, deviations from this basic model have long
50 been documented, in particular for mid-oceanic ridge samples (Chauvel and BlichertToft, 2001;
51 Debaille et al., 2006; Patchett and Tatsumoto, 1980; Salters and White, 1998). For example, a lack of
52 correlation between these two systems characterizes MORBs collected between 22°N and 35°N
53 (Debaille et al., 2006). Anomalously high values of $^{177}Hf/^{176}Hf$ for a given $^{143}Nd/^{144}Nd$ have also
54 been measured along Mohns ridge (Blichert-Toft et al., 2005). These deviations from the mantle
55 array model were initially interpreted as the result ofisotopic disequilibrium between melts and their
56 mantle source across the garnet-spinel transition beneath the mid-oceanic ridge (Blichert-Toft et al.,
57 2005; Debaille et al., 2006). More recently, a systematic study of Hf-Nd isotopes in oceanic basalts
58 has shown an array of parallel trends on a global scale (Salters et al., 2011). These authorsattributed
59 these sub-parallel arrays to the involvement of varying amounts of highly residual peridotites within
60 the upper mantle. According to this model, the non-uniformity of the depleted component together
61 with the lack of fine-scale sampling could explain the lack of correlation between εHf and εNd along
62 the global mid-oceanic ridge system.

63 In the central part of the Lucky Strike ridge segment along the Mid-Atlantic Ridge (MAR), the
64 exceptional sampling resolution gives an opportunity to examine the different hypothesese for Lu-Hf
65 and Sm-Nd isotope systematics in the mid-oceanic ridge environment at a local scale. A recently
66 published petrogenetic model for this area has shown the existence of significant geochemical
67 variations in the Lucky Strike segment mantle source (Gale et al., 2011). Based on this study, we
68 have selected a suite of representative samples spanning the whole range of geochemical variation
69 and located within an $8km^2$ in the central portion of the segment. The Lucky Strike segment is also
70 proximal to, and influenced by the Azores hotspot (Dosso et al., 1999; Langmuir et al., 1997;
71 Schilling, 1975). Therefore, our new sample collection can also provide new constraints on the origin
72 of the geochemical anomaly associated with the Azores hot spot-MAR interaction.

2. Geological setting and small scale sampling

The area studied is located along the MAR, South-West of the Azores triple junction. Geochemical evidence together with geomorphological and geophysical characteristics demonstrate a clear plume-ridge interaction in this region (Asimow et al., 2004; Gale et al., 2011; Gente et al., 2003; Schilling, 1975). In this area, the MAR is characterized by a succession of segments bound by left-lateral, non-transform offsets. The Lucky Strike segment (fig. 1) is 60 km-long and bound by non-transform discontinuities at 37°00'N and 37°35'N. It is a slow ridge segment characterized by a full spreading rate of 21 mm/yr. This segment, located south west of the Azores hotspot, is significantly shallower and volcanically more robust than other MAR segments (Cannat et al., 1999; Escartín et al., 2001). The axial lithospheric structure and composition are typical of slow spreading ridges, characterized by a well-developed, 11-12km-wide axial valley, and a deepening of 1600m of the valley floor towards the segment ends (Detrick et al., 1995) where serpentinized peridotites outcrop (Gràcia et al., 1997). The prominent seamount at the segment center (the Lucky Strike volcano) is 7km wide and 15km along axis. It is underlain by an axial magma chamber 3.4km below the seafloor (Singh et al., 2006) and hosts an active hydrothermal field at its summit (Langmuir et al., 1997). Several volcanic ridges spread north and south from this central volcano suggesting along axis diking, while magnetic data suggest that magmatic accretion in the center of the Lucky Strike segment is presently focused in a narrow graben at the top of the central volcano (Miranda et al., 2005). This area has been well studied since the hydrothermal field discovery in 1992 (Langmuir et al., 1997), with a uniquely dense sampling among slow-spreading segments; more than 200 basaltic samples have been collected with dredges, wax cores, submersibles, and other deep-sea vehicles. Sample distribution along the segment is uneven, with the highest density on the central volcano. We report here new Sr, Nd, Pb and Hf isotopic data for 18 samples collected there during the

Graviluck06 and Bathyluck09 cruises (Table 1), using the Nautile submersible (IFREMER) and Remotely Operated Vehicles (Victor; Figure 1).

3. Analytical methods

Trace elements were measured using the Brucker 820 ICP-MS quadrupole instrument at the Laboratoire de Planétologie et de Géodynamique in Nantes. Dissolutions were performed on 50 mg of sample at a temperatures of 120˚C for 12 hours in 1 mL 8N HNO_3 and 0.5 mL ~23N HF. Samples were evaporated to dryness at 80˚C, then re-dissolved in 2mL 8N HNO_3 and re-evaporated. The final dissolution was made in 4 mL 4N HNO_3 before a 1:5000 dilution in 0.3N HNO3. Ge, Rh, In, Tm and Bi were used for internal standard normalization and the following standards were used for calibration curves: BHVO-2, W2, DNC-1, BIR-1 and the LDEO (Columbia University) in-house standard Mid-Atlantic Ridge basalt MAR. The LDEO in-house standard K1919, collected from the same lava flow as BHVO-1, was also analyzed several times within each analytical run to correct for instrumental drift. The continental basalt reference material BR, from the CRPG Nancy was analyzed several times to test our analytical reproducibility. All data are reported in table 1.

For isotope measurements, powdered samples (400-700 mg) were dissolved in Savillex vials with concentrated HF-HBr ultrapure acids (3:1 in volume). Pb, Hf, Sr and Nd were separated from the same dissolution using four different columns starting with Pb to minimize contamination. The Pb extraction technique used was from (Manhes et al., 1978), using HBr 0.5M and HCl 6M on AG 1-X8 anion resin. Pb blanks measured using this procedure were < 100 pg, and thus are negligible relative to the amount of sample analyzed. The effluent containing Hf, Sr and the rare earths were evaporated and taken up in 6M HCl, evaporated again and taken up in 1 ml of 0.5M HCl/0.15M HF. It was then ready to pass through an AG 50-X8 cation column (microcolumn Savillex, 30 ml, 6.4mm ID x 9.6mm OD x 25 cm). The first 6 mls containing the Hf-Ti fraction were eluted in 0.5M HCl/0.15M

HF. The rest of the elution was completed using 3M HCl to separate Rb from Sr and 4M HNO_3 to separate Ba from rare earths. Nd was separated from Ce and Sm using 0.2M HCl and 0.35M HCl on a 0.8x4cm Biorad column loaded with LN Eichrom resin. The Hf-Ti fraction was evaporated and taken up in 6M HCl with a few µl of H2O2. It was loaded on a column made of a pipette tip filled with 100 mg of LN Eichrom resin. Ti was first eluted with 10ml 6M HCl with 50µl of H_2O_2 and Hf was collected in 5 ml of 2M HF.

Sr isotope ratio measurements were carried out by thermal ionization mass spectrometry using a Finnigan Mat26x and a Thermo Finnigan Triton. Compositions were normalized for instrumental mass fractionation relative to $^{86}Sr/^{88}Sr = 0.1194$. $^{87}Sr/^{86}Sr$ of the NBS987 Sr standard during the course of the analyses yielded 0.710235 ±45 (n=4, 2σ) for the MAT26x and 0.710255 ±20 (n=2) for the Triton. Isotopic compositions of Hf and Pb were measured at Ifremer, Brest, using a MC-ICPMS Neptune. Repeat measurements of the Hf isotope standard JMC 475 (Denver) during the course of the analyses yielded $^{176}Hf/^{177}Hf = 0.282145 \pm 13$ (n=8, 2σ). The results were normalized to the value of 0.282158 using $^{179}Hf/^{177}Hf = 0.7325$ for mass fractionation correction. The Pb isotope data are reported relative to published values for NBS 981 (Catanzaro et al., 1968). The samples were spiked with thallium to correct for mass fractionation. Based on repeated runs of NBS 981, the estimated external precision for Pb analyses is ±0.02%, 2σ for $^{206}Pb/^{204}Pb$ and $^{207}Pb/^{204}Pb$ and ±0.03%, 2σ for $^{208}Pb/^{204}Pb$. During the course of the analyses, 10 replicates of the Pb isotope standard NIST981 gave an average of 16.930 ±0.003 (2σ) and 15.482 ±0.003 (2σ) and 36.668 ±0.008 (2σ) for $^{206}Pb/^{204}Pb$, $^{207}Pb/^{204}Pb$ and $^{208}Pb/^{204}Pb$ respectively. Isotopic compositions of Nd were measured at Institut Universitaire Européen de la Mer, Brest, using a Thermo Finnigan, Triton. The measurements were carried out in static mode. All Nd data are fractionation corrected to $^{146}Nd/^{144}Nd=0.7219$. During the course of the study, analyses of the La Jolla standard were performed and gave an average of $^{143}Nd/^{144}Nd = 0.511843 \pm 4$ (n=4 2σ).

Using the same analytical method, BCR-2 gave values of $^{176}Hf/^{177}Hf$ = 0.282861 ±9, $^{206}Pb/^{204}Pb$ = 18.7496 ±7, $^{207}Pb/^{204}Pb$ = 15.6175 ±7, $^{208}Pb/^{204}Pb$ = 38.7291 ±21, $^{87}Sr/^{86}Sr$ = 0.705008 ±8, $^{143}Nd/^{144}Nd$ = 0.512629 ±8.

4. Results, geochemical variations in Lucky Strike basalts

The Lucky Strike segment contributes to the definition of the general geochemical gradient South of the Azores (Dosso et al., 1999; Gale et al., 2011; Langmuir et al., 1997; Schilling, 1975). Samples from this area have long been characterized as enriched in incompatible elements compared to normal-MORB with La_N/Sm_N and K_2O/TiO_2 ratios higher than 1.25 and 0.11 respectively. Our data are in good agreement with this first order observation. Lucky Strike samples show varying levels of incompatible element enrichment, with a bi-modal distribution of K_2O/TiO_2 ratios (Fig. 2a). We have defined two different groups named "transitional-MORB" ($0.11 < K_2O/TiO_2 < 0.25$) and "enriched-MORB" ($K_2O/TiO_2 > 0.25$), consistent with the definitions in Gale et al. (2011). These two groups also show different petrographic characteristics: transitional-MORB samples are fresh aphyric basalts, whereas enriched-MORB samples are slightly altered vesicular basalts with plagioclase (0-20%) and olivine (0-3%) phenocrysts. Groundmass textures are microcrystalline for E-MORB samples and vary from microcrystalline to glassy for T-MORB samples.

Basalts from the transitional group are found throughout the segment whereas enriched basalts are found almost exclusively in the center. Our samples were recovered solely in the central part of the segment within an area of less than 8 km^2. They display $1.25 < La_N/Sm_N < 2$ typical of transitional MORB (9 samples) and $La_N/Sm_N > 2$ typical of enriched MORB (9 samples) showing therefore the entire range in incompatible element enrichment previously reported for the whole Lucky Strike segment (Gale et al., 2011) (Fig. 2a). Figure 2b presents the REE patterns normalized to chondritic CI values for both groups of samples. Transitional samples are characterized by relatively flat REE

patterns with slight enrichments in light REE, whereas enriched samples have marked enrichments in light REE (60-70x chondrites) and show slight fractionations between middle and heavy REE. It is worth noting that samples from the Eastern slopes of the central volcano and from the Eastern axial valley wall (named GRA-Nxx) show the same range of variation as that from samples collected exclusively on the summit of the Lucky Strike volcano (named B09-ROCxx). This indicates that the patterns described here do not reflect a temporal variability of basalt compositions at time scales of about 500 ka (spreading age of the sample furthest from the axis) or less. Sr, Nd and Pb isotopes show variations that are in good agreement with previous data from this ridge segment (Gale et al., 2011). The most enriched samples exhibit coherent, more radiogenic Pb, Sr and less radiogenic Nd than the intermediate group (fig. 4). In binary isotope diagrams, Lucky Strike samples plot along mixing lines between a depleted mantle component and an enriched component attributed to the Azores hotspot. In these isotopic dimensions, even the less enriched samples from Lucky Strike are significantly more enriched than the DMM, which agrees with their major and trace element compositions. A simple mixing model between the DMM (Salters and Stracke, 2004) and the Azores mantle (Beier et al., 2007) reproduces the variations in $^{207}Pb/^{204}Pb$, $^{206}Pb/^{204}Pb$ and εNd, $^{87}Sr/^{86}Sr$.

Our new dataset shows a range of values from εHf = +14.3 to +22.1, comparable to values previously reported in ridge segments immediately South and North of Lucky Strike (Agranier et al., 2005; Chauvel and BlichertToft, 2001). Despite the limited spatial extent of our sampling area, the new data show a range of variation that is of the same order of magnitude as that reported for the entire MAR (Agranier et al., 2005; Andres et al., 2004; Debaille et al., 2006). It is worth noting that the transitional group extends towards a more radiogenic εHf end-member in the Hf-Nd isotopic diagram and therefore plots above the mantle array. In contrast, in the same diagram, the enriched group extends toward a lower εHf end-member and plots near the Azores isotopic field, below the mantle array (fig. 5). The positive correlation between εHf and εNd agrees with the expected

coherence of Sm-Nd and Lu-Hf isotopic systems during magmatic processes, albeit with an unusual slope compared to that of the mantle array (Fig. 5). Compared to other isotopic systems, the systematics of Hf isotopes in this region of the MAR are still poorly known (fig. 3), and the Hf isotopic ratios reported here are the first for the Lucky Strike segment. Basalts collected along the MAR between 46° to 35°N reveal a comparable slope, however, (Agranier et al., 2005; Chauvel and BlichertToft, 2001; Dosso et al., 1999; Salters et al., 2011; Yu et al., 1997) which is strikingly different from the Nd-Hf correlation observed along other regions of the MAR (Fig. 5). The Hf versus Sr isotope diagram shows a similar abnormal correlation compared to the rest of the MAR. We additionally observe that the Lucky Strike transitional end-member seems relatively radiogenic in Pb isotopes ($^{206}Pb/^{204}Pb > 19.35$) compared to the classical depleted mantle (Salters and Stracke, 2004) ($^{206}Pb/^{204}Pb \approx 18.20$) (Fig. 5a).

This unusual isotopic signature is however not unique in MORB, having been detected, for example, in basalts from Mohns Ridge (fig. 6). The most depleted samples from this northern Atlantic ridge show values of εHf for a given εNd to be very similar to those of Lucky Strike samples (Blichert-Toft et al., 2005) (Fig. 6). However, important differences exist between the two zones: (i) Mohns Ridge samples define a hyperbolic εHf- εNd array instead of the linear Lucky Strike trend (Blichert-Toft et al., 2005), (ii) values of Pb isotopic ratios in depleted Mohns Ridge samples are unradiogenic ($^{206}Pb/^{204}Pb \approx 17.95$) and (iii) a geographical trend is present along Mohns Ridge, whereas the Lucky Strike variability is observed within a small (< 8 km^2) area on axis, and reproduced in basalts from other segments in the 45-35°N MAR region near the Azores.

5. Discussion

5.1 Significant geochemical variations in basalts at local scale.

5.1.1. Small scale mantle heterogeneities or disequilibrium melting?

At this fine sampling scale, it is important to investigate whether the geochemical variations observed in basalts are the result of mantle heterogeneity or if they are produced by kinetic processes during melting. Early studies have commonly observed a wide range of εHf in MORB for a given εNd, leading to the hypothesis that melts may not be isotopically equilibrated with their peridotitic sources (Blichert-Toft et al., 2005; Debaille et al., 2006). According to this hypothesis, a highly variable Hf isotope dataset may result from the disequilibrium melting of a garnet-bearing peridotite in which the individual mineral phases are not in isotopic equilibrium (Blichert-Toft et al., 2005; Debaille et al., 2006). Because garnet incorporates Lu preferentially over Hf, it could develop a time-integrated signature with elevated εHf values. Preferential melting of garnet would therefore likely produce highly radiogenic Hf values in basalts. Hf^{4+} is expected to possess a lower diffusion coefficient than Pb^{2+} and Nd^{3+}, which could explain why this element would be more sensitiveto this kinetic process. If the isotopic composition of a particular mineral phase dominates the isotopic composition of the generated melt, variable εHf compositions in MORB may be generated from a single mantle domain during the current melting event below the present-day ridge. In this hypothesis, the local depleted mantle identified on εHf diagrams (fig. 5) may not correspond to a real end-member, but may instead result from a deviation toward radiogenic εHf values due to kinetic processes during mantle melting. This disequilibrium melting hypothesis has been proposed to explain the high εHf component found along Mohns and Knipovich ridges (Blichert-Toft et al., 2005) (fig. 6), and to explain the lack of correlation between εHf and other isotopes systems along the MAR between 22 and 35°N (Debaille et al., 2006).

233 Several arguments lead us to rule out this kinetic hypothesis as the cause of observed εHf
234 variations at Lucky Strike. A primary line of evidence stems from the good correlation between εHf
235 and other isotopic systems, which is not expected if kinetic processes influenced this isotopic ratio.
236 An assumption of the disequilibrium melting hypothesis is that partial melting takes place in presence
237 of garnet, which is irreconcilable with geochemical characteristics of the Lucky Strike transitional
238 basalts that do not show any fractionation between medium REE and heavy REE as would be
239 expected if melting occurs in the garnet stability field (Fig. 2b). This conclusion is in good agreement
240 with a recent petrogenetic model of melt supply to the Lucky Strike segment based on basalt
241 geochemistry, indicating that melting is controlled by spinel peridotite for the transitional group
242 (Gale et al., 2011). As recently demonstrated by Salters et al., (2011), a second line of argument
243 against disequilibrium melting is based on experimental studies of diffusion coefficients in garnet. In
244 this particular mineral, Dy diffusively equilibrates over 1 mm in 100,000 years at 1400°C (Van
245 Orman et al., 2002). Even if we consider a diffusion coefficient 10 times slower for Hf^{4+},centimeter-
246 scale isotopic equilibrium at mantle temperatures is expected to take place over one or two million
247 years. This equilibration time is orders of magnitude shorter than the time needed to build up a
248 radiogenic Hf signature. Disequilibrium melting is thus not a plausible hypothesis to explain the
249 unusually radiogenic Hf characteristic of the most depleted component along Lucky Strike.

250 If melting takes place at isotopic equilibrium, the Hf isotope composition of the melt is controlled
251 by the whole rock composition of the peridotite. The presence or absence of garnet in the residual
252 assemblage of the current melting event is therefore irrelevant and the source itself must have an
253 anomalous isotopic signature.

254 5.1.2. Small scale mantle heterogeneity and efficiency of magma mixing.

Our study of a high spatial resolution dataset (<5 km) reveals the existence of incompletely mixed coexisting primary magmas in the erupted material, despite the melt lens imaged at 3.4 km below the seafloor (Singh et al., 2006). At first glance, the large variations measured in lithophile element isotopic systems are in conflict with the lack of variation in He and Ne isotopes measured on samples from the same cruises (Moreira et al., 2011). Because noble gas analyses require perfectly fresh glass, He and Ne measurements have been conducted on a slightly different subset of Graviluck06 and Bathyluck09 sampling, excluding samples from the more enriched group. This sampling bias can partly explain the observed discrepancy. However, even within the transitional group of Lucky Strike samples, Sr, Nd, Pb and Hf isotopes illustrate small variations that are not seen in He isotopes. We propose that this difference is explained by the difference of diffusivity in melt between heavy radiogenic isotopes and noble gases. The small-scale geochemical variations of trace elements and Sr, Nd, Pb and Hf isotopes indicate that neither the magma chamber nor the magmatic plumbing system totally homogenize the melts, therefore preserving, at least partially, the local mantle heterogeneity signal. These compositionally distinct liquids can be produced simultaneously if the scales of geochemical heterogeneities in a marble-cake assemblage are smaller than the melting zone. Beneath the Lucky Strike central volcano, we know that the melting column extends 80 km below the seafloor. In addition, geophysical evidencehas shown that the focusing of melts toward the centers of segments is common along slow-spreading segments (Detrick et al., 1995), and thus sampling at the segment center can reflect mantle composition at a larger scale. Depending on the efficiency of along-axis melt migration, the volume of mantle tapped by the magmatic body could extend up to the whole ridge segment (70 km at Lucky Strike). This length-scale represents, therefore, an upper limit for the size of geochemical heterogeneities in the marble-cake assemblage. Within the compositional heterogeneity of the Lucky Strike dataset, the atypical Hf isotopic signature is only shown by the transitional group. This observation suggests that this mantle signature is carried by the local, more refractory, mantle component. This high εHf signature is absent in Azores' islands basalts, most

likely due to the difference of lithospheric thickness between the two geological settings (> 50 km beneath São Miguel and ≈ 10 km beneath the ridge); continuation of melting to shallower levels beneath a thin lithosphere allows for a higher degree of melting and thus allows for a greater proportion of melts to derive from the more refractory mantle component. Our study also implies that interpretation of large- scale sampling of mantle domains using inadequate sample spacing should be approached with caution. As shown recently by Salters et al. (2011), the long believed lack of correlation between εHf and other isotope systems along mid-oceanic ridges is likely the result of a sampling bias and scarcity of data at a fine scale.

5.2 Origin of the mantle component with anomalous high εHf.

According to a recent petrogenetic model based on major and trace element compositions and Sr, Nd and Pb isotopes, the source of Lucky Strike transitional basalts (called "local DM" in figures 5, 6 and 7) results from a mixing between a DMM-like end member and a metasomatized mantle with an isotopic composition similar to Azores mantle (Gale et al., 2011). However, since the Azores lavas have a εHf-εNd composition below the mantle array, simple mixing cannot account for the high εHf values (+24) and relatively low εNd values (+10) measured in the transitional group (fig. 5).

5.2.1 Ancient, residual mantle component.

It has long been suggested that Hf-Nd isotope decoupling in the mantle source can be produced by an ancient melting event involving garnet fractionation, and subsequent melting of the resulting mantle residue (Blichert-Toft and Albarede, 1997; Chauvel and BlichertToft, 2001; Salters and Hart, 1989; Salters and Zindler, 1995). Because the ratio of Lu and Hf partition coefficients between garnet and a basaltic liquid ($K_D{}^{Lu}_{Grt-liq}/K_D{}^{Hf}_{Grt-liq}$) is very high (> 30), mantle residues produced by melt extraction at great depth would likely be HREE-enriched relative to Hf. An ancient partial melting event in the garnet stability field should yield a high $^{177}Hf/^{176}Hf$ signal in the residue, and the

amplitude of this signal should increase with the time elapsed since the melting event. In contrast, Sm and Nd have similar partition coefficients in garnet and spinel peridotite and εNd is therefore expected to remain almost unaffected by the two different types of melting events. Given a sufficient length of time (1-2 Ga), the residual garnet peridotite should therefore develop an isotopic signature characterized by a steeper slope in εHf versus εNd diagram. This interpretation is consistent with the mixtures of variously-depleted mantle model proposed by Salters et al. (2011) to explain the array of sub-parallel trends of Hf-Nd isotope ratios in oceanic basalts on a global scale. According to this model, ancient residual oceanic lithosphere (ReLish, Salters et al., 2011), produced by the extraction of the crust, is recycled and mingled into the MORB and/or OIB mantle sources. Is the ReLish a possible component of the Lucky Strike mantle assemblage?

As mentioned earlier, the recently published petrogenetic model for Lucky Strike basalts (Gale et al., 2011) does not fit the unusual εHf-εNd correlation obtained for our samples. This model can briefly be summarized by a 2-step geochemical history: i) mixing between the DMM (90%) and the Azores mantle (10%), and ii) metasomatism by low-degree melts produced in the garnet stability field in the Azores mantle. The first step defines the regional gradient along the MAR South of the Azores, whereas the second step generates the local variability shown by transitional and enriched groups. We attempted to adjust this petrogenetic model and we replaced the DMM component with a mixture between DMM and ReLish. This latter component is highly depleted and almost completely exhausted of incompatible elements, and its signatures can easily be overpowered by a small addition of enriched components. This could explain why the influence of the ReLish component is not observed on highly incompatible isotopes system (Rb-Sr, U,Th-Pb). We have modeled the trace elements (REE+Hf) together with the Sr-Nd-Pb-Hf isotope compositions of Lucky Strike basalts. The details of the melting models are in the supplementary material and results can be seen on figure 5, 6 and 7. In this model, the ReLish component was produced 1.2 Ga ago, by a 6% melting event in the

garnet stability field, from a MORB source that has been isolated from the bulk silicate Earth reservoir for 2 Ga. We are able to reproduce the trace element and isotopic systematics of Lucky Strike basalts by a two-steps model: i) mixing of 20% of the ReLish component to a mantle assemblage of DMM (70%) and Azores mantle (10%), and ii) a metasomatism of this local Lucky Strike mantle by low-F melts produced in presence of garnet from the Azores mantle. This solution is not unique and it is possible to fit the data with a different set of parameters. For example, the mass fraction of the ReLish component is inversely proportional to its formation age: a more recent ReLish would simply imply a greater proportion in the mantle assemblage. Our goal is therefore not to quantify these melting events accurately, but rather to show that the presence of a ReLish component in the source of Lucky Strike basalts is able to produce the atypical high εHf end-member (Fig. 6). The presence of such refractory component could also explain the relatively low degree of melting (7%) calculated by Gale et al. (2011) for the present day melting beneath the ridge. Although residual oceanic lithosphere material is probably a ubiquitous mantle component, due to its refractory properties, it is expected to contribute little to the observed global MORB variations.

5.2.2 Sub-continental lithospheric mantle.

A second potential candidate for the atypical source signature in Lucky Strike transitional basalts is the Sub-Continental Lithospheric Mantle (SCLM). Compositions of the SCLM are primarily based on xenolith and xenocryst samples. These samples show a large range of Hf isotopic compositions up to very radiogenic values (Simon et al., 2007). This variability in Hf isotopes is associated with less variable and less radiogenic Nd isotopic compositions.composition The SCLM consists mainly of ultramafic rocks, ranging from lherzolites to dunites. Despite the observed petrological diversity of this reservoir, a recent tomographic study has suggested that most Archean sub-continental lithospheric mantle originally consisted of depleted dunites and harzburgites (Griffin et al., 2009). In intraplate volcanic areas, these refractory peridotites are subsequently metasomatized and refertilized.

In xenolith datasets, the decoupling between Hf and Nd isotopes in this subcontinental reservoir has been interpreted as a result of depletion events followed by carbonatite-type metasomatism (Simon et al., 2007). This process is expected to link very radiogenic εHf values with relatively less radiogenic Nd and enrichment in highly incompatible trace elements, consistent with the geochemical characteristics of the transitional Lucky Strike basalts (Fig. 5).

Several studies have argued for contamination of the MORB source by either the crustal or the mantle part of the continental lithosphere (e.g. Hanan et al., 2004; Janney et al., 2005). Because the Rb/Sr ratio is very high in the continental crust, addition of this material to the depleted mantle would dramatically increase $^{87}Sr/^{86}Sr$ values. In contrast, the mantle portion of the continental lithosphere is not expected to have an exceptionally high Rb/Sr ratio and is therefore a more likely component. The presence of relics of SCLM preserved in the upper mantle in the North-central Atlantic area has been a matter of debate for the last 15 years. For example, SCLM is suspected to explain the distinctive metasomatic parageneses and garnet signature in spinel-peridotite xenoliths from Cape Verde Archipelago (Bonadiman et al., 2005). Similarly, the enriched component in the lavas from São Miguel has been inferred to contain a contribution from localized pieces of SCLM material (Madureira et al., 2011; Moreira et al., 1999; Widom et al., 1997). According to these studies, this sub-continental lithospheric mantle originally resided beneath North-western Africa or Iberia and was delaminated during rifting upon the opening of the Atlantic Ocean basin. However, based on the low εHf measured in lavas from Azorean islands, other studies have argued against this hypothesis (Beier et al., 2007; Elliott et al., 2007). In contrast to these studies, we propose that SCLM material is a potential candidate for the origin of the transitional group basalts, and should be seen as a possible refractory component of the mantle rather than the source of the enriched basalts. As previously discussed in §5.1.2, this is in good agreement with the fact that this signature is exclusively observed

374 at the ridge axis, where the shallower melting compared to Azores islands allows more refractory
375 material to melt.

376 It is important to note that the geochemical composition of the SCLM remains poorly constrained.
377 It is therefore difficult to produce an incontrovertible mixing model involving this reservoir. SCLM
378 samples show highly heterogeneous isotopic signatures, which seems to be inconsistent with the
379 tightly defined nature of the more depleted Lucky Strike end-member. However, based on our
380 present day knowledge of the Hf-Nd isotope characteristics of SCLM xenoliths, the addition of this
381 type of material to the Lucky Strike upper mantle could account for the abnormal isotopic signature
382 of the local depleted end-member.

383 Distinguishing whether the abnormal Hf-Nd isotopic signature is the result of the presence of
384 residual oceanic lithosphere previously melted in the garnet stability field (*i.e.* ReLish) (§5.2.1) or the
385 contribution of sub-continental lithospheric mantle (§5.2.2), is not straightforward. Very ancient
386 depleted signatures in Os isotopes have long been suggested as a characteristic of subcontinental
387 lithospheric mantle. But recent studies of abyssal peridotites have shown a wide range of $^{187}Os/^{188}Os$
388 ratios at slow mid-oceanic ridge settings extending to very unradiogenic values (Liu et al., 2008). If
389 highly depleted Os isotope signatures are not unique to the SCLM, there are no isotopic or chemical
390 signatures that unambiguously distinguish the two proposed hypotheses.

391 ## 5.3. Geodynamical implications.

392 We have shown that the unusual Hf isotope signature in basalts from Lucky Strike is best
393 explained by the melting of a refractory component in the mantle near the Azores rather than by a
394 kinetic effect during the current melting event. Even if we cannot specify whether this refractory
395 component is a ReLish or a SCLM, we have shown that this component is mixed with the depleted
396 mantle and the Azores mantle prior to the addition of the metasomatic agent (low-F melts derived

397 from the Azores; Gale et al., 2011). The existence of this component and its mixing relationship raise
398 the question of the structure of the upper mantle around the Azores.

399 Since only limited data are available for Hf isotopes compared to other isotope systems, it is not
400 possible to map precisely the extent of the particular Hf signature recognized in our local scale study.
401 However, the Nd vs. Hf isotopes of segments North and South of the Lucky Strike segment show a
402 similar correlation (fig. 5). The latitudinal extension of this atypical correlation is therefore at least
403 between 46°N to 35°N, and centered at the latitude of the Azores hotspot. This along-axis extension
404 is significantly shorter than the regional gradients defined by Sr isotopes or La/Sm ratios (Dosso et
405 al., 1999; Gale et al., 2011; Langmuir et al., 1997; Schilling, 1975). By analogy to observations along
406 the MAR near Ascension Island (Paulick et al., 2010), the hypothesis involving mixing between one
407 enriched component and two different depleted components (DMM and ReLish/SCLM) is expected
408 to produce a cloud or two different trends in Nd-Hf isotope diagrams. Since only one trend is seen
409 from 46°N to 35°N (Agranier et al., 2005; Chauvel and BlichertToft, 2001; Dosso et al., 1999; Yu et
410 al., 1997) (fig. 4), we can infer that the depleted components in the system are well homogenized.

411 A first possible model for the upper mantle structure in the Lucky Strike and Azores domain is
412 that the refractory mantle component is a primary constituent of the Azores hotspot, mixing with the
413 regional mantle (fig. 8A). In this hypothesis, this refractory component has been recycled in the
414 asthenosphere and brought back to the surface by the hotspot. The initial depletion event could either
415 be the result of deep ancient melting in an oceanic domain (ReLish) or of some mantle material from
416 the base of the continental lithosphere (SCLM) which was recycled deep in the mantle.

417 An alternative model is an upper mantle constituted of different coexisting refractory materials
418 prior to the arrival of the Azores plume (fig. 8B). In this hypothesis, the atypical depleted component
419 could be a ubiquitous residual mantle component (*i.e.* ReLish) or relics of the SCLM left behind by

the North-East drifting of the African continent (fig. 8B). The presence of the particular isotopic signature in the transitional Lucky Strike samples could be the result of a change of the melting regime near the Azores (Asimow et al., 2004; Schilling, 1975). Between 46˚N and 35˚N, the thin lithosphere and the local increase of mantle potential temperature (Asimow et al., 2004; Schilling, 1975) (+ 35˚C) associated with the thermal influence of the Azores enhances mantle melting. These pressure and temperature conditions would allow melting of the more refractory mantle identified around the Azores region. Future Hf-Nd studies along segments near Lucky Strike will provide constraints on the geographical extension of this refractory component and allow study of the along-axis evolution of its mixing proportions with the ambient mantle.

6. Conclusion

We report a strong correlation between Hf and Nd isotopic systems from MORBs within the Lucky Strike segment along the MAR, which is contrary to the commonly accepted decoupling of these systems. In good agreement with recent results by Salters et al. (2011), our results suggest that the lack of correlation between εHf and other isotope systems along the global mid-oceanic ridge system is the result of sampling bias. Part of the reason for not observing more segments with correlated Hf-Nd isotope systematics may be the lack of fine-scale, dense sampling. In order to discuss the origin and significance of large-scale mantle composition, alternative solutions are (i) high spatial resolution sampling of the ridge or (ii) statistical techniques such as spectral analyses (Agranier et al., 2005), where the dataset interpretation is weighted by the sampling density.

The Hf-Nd isotope correlation seen in Lucky Strike samples is significantly different from the global mantle array defined by MORB and OIB, and is characterized by an unusually high εHf values for a given εNd. In every binary isotopic plot, Lucky Strike basalts define a trend from this atypical radiogenic Hf mantle component toward the Azores enriched mantle. We have shown that kinetic

443 effects cannot account for the observed Hf-Nd systematics in Lucky Strike basalts and that this trend
444 is best explained by mixing enriched and depleted components in the local mantle. If the origin of the
445 enriched component is clearly related to the Azores hotspot, the origin of the depleted mantle source
446 is more controversial. We propose that this unusual end-member could either indicate the presence of
447 some residual oceanic lithosphere or some sub-continental lithospheric mantle left behind by the
448 drifting of the African continent. At Lucky Strike, enhanced melting conditions associated with the
449 Azores plume allow us to detect this refractory component within basalts erupted on-axis. This
450 observation points towards the existence in the mantle of domains of refractory material that do not
451 melt in normal mid-oceanic ridge conditions, thus contributing little to the global MORB
452 compositions. This study emphasizes the heterogeneous nature of the depleted mantle long
453 considered the archetype of a homogeneous mantle domain.

454

455 # Acknowledgements

456 This study was funded by the CNRS-INSU, ECORD and partial support was provided by ANR
457 (France) Mothseim (project NT05-3 42213). We gratefully acknowledge Valerie Ballu and the
458 science party of the Graviluck expedition. We thank Emmanuel Ponzevera, Philippe Nonnotte, Claire
459 Bassoulet, Céline Liorzou and Carole La for their technical assistance, and Catriona McCabe for her
460 help with the manuscript. We acknowledge Laurie Reisberg for the editorial handling, Vincent
461 Salters and an anonymous reviewer for constructive comments. This is IPGP contribution #xxx.

462

Figure captions

Figure 1: Bathymetric maps of (A) the Mid-Atlantic Ridge, (B) Lucky Strike segment and (C) Arctic ridges. Locations of our new samples (square symbols) are shown together with published samples: of the entire MAR (gray circles), the Azores geochemical anomaly (yellow circles) and Mohns ridge (green triangles). Symbols are the same in all the figures, published data are from (Agranier et al., 2005), (Andres et al., 2004; Andres et al., 2002), (Blichert-Toft et al., 2005), (Castillo and Batiza, 1989), (Chauvel and BlichertToft, 2001), (Debaille et al., 2006), (Dosso et al., 1993; Dosso et al., 1999; Dosso et al., 1991), (Douglass et al., 1999), (Frey et al., 1993), (Fontignie and Schilling, 1996), (Hamelin et al., 1984), (Hanan et al., 1986), (Ito et al., 1987), (Machado et al., 1982), (Nowell et al., 1998), (Paulick et al., 2010), (Salters, 1996), (Schiano et al., 1997), (Schilling et al., 1994), (Shirey et al., 1987), (Yu et al., 1997).

Figure 2: A) histogram showing the bimodal distribution of Lucky Strike samples. Two distinct peaks define the two petrological groups described in this study: "Transitional" if $K_2O/TiO_2 < 0.25$ and "enriched" if $K_2O/TiO_2 > 0.25$. Data are from this study together with unpublished data (Bezos personal communication), Gale et al. (2011) and Ferreira (2006). B) Diagram showing normalized REE concentration of the two groups.

Figure 3: Geochemical gradient south of the Azores. The center of Lucky Strike segment shows a large range of geochemical variation.

Figure 4: Binary isotopic plots showing Lucky Strike data compared to previously published MAR and Azores data. Mixing models between a depleted (DMM, (Salters and Stracke, 2004)) and an enriched (Azores, Gale et al., 2011)) components are shown. The chosen Azores mantle composition assumed is that of the least enriched end-member (Sete Cidades samples, Beier et al. (2007)).

Figure 5: Hf isotopes versus other isotopic systems. The model modified from (Gale et al., 2011) is shown as black lines. Small dark squares along these lines represent percentage of low-F melts additions (1% step) to the local Depleted Mantle (Local DM, see text for further explanations). Compare to the mantle array, new data from Lucky Strike segment define a trend with very radiogenic Hf composition for a given εNd. The same atypical correlation can be observed along the MAR in samples collected between 46 and 35°N (yellow circles).

Figure 6: Comparison between Lucky Strike data and Mohns ridge sample, previously described as geochemically abnormal with εHf for a given εNd. The same model shown in figure 5 is reported here, fractions of low-F melts added to the regional mantle are shown in percent.

Figure 7: Hf isotopes versus La/Hf, and Nd isotopes versus La/Nd. Metasomatism of the regional mantle by low-F melts allow to reproduce the geochemical heterogeneity measured at Lucky Strike.

Figure 8: Two different models for the structure of the upper mantle near the Azores. In the left column, the atypical depleted component is a primary constituent of the Azores hotspot. In the right column, this component resides in the upper mantle prior to the plume arrival.

Supplementary figure: Lu/Hf vs Sm/Nd diagram. Green and orange lines represent melting models (batch and fractional) with residual spinel and residual garnet, respectively. The black line represents low-F melts metasomatism model (see text for further explanations). The Lucky Strike abnormally high Lu/Hf ratio for a given Sm/Nd ratio is well explained by the influence of this recent metasomatism event.

Table 1: Major element, trace element and isotopes data for samples collected at Lucky Strike segment center. AII127-D15G has previously been published in Dosso et al. (1999), except new Pb

508 and Hf isotope measurements done on a MC-ICPMS at SDSU in collaboration with Barry Hanan. [b]
509 Sr isotope measured using a Thermo Finnigan Triton. [c] Sr isotope measured using a Finnigan
510 MAT26x.

511

Table 1

Sample	AII127-D15G	B09-ROC01	B09-ROC07	B09-ROC08	B09-ROC11	B09-ROC13
Long. (°)	-32.283	-32.282	-32.282	-32.282	-32.277	-32.276
Lat. (°)	37.291	37.284	37.291	37.291	37.297	37.299
Type	T-MORB	E-MORB	T-MORB	T-MORB	E-MORB	E-MORB
SiO_2	51.4	49.3	51.4	51.5	48.8	50.1
TiO_2	1.07	1.08	1.05	1.05	1.28	1.20
Al_2O_3	14.7	17.0	14.8	15.1	16.4	16.7
FeO	9.8	6.4	9.9	9.5	7.5	6.8
MnO	0.18	0.12	0.18	0.19	0.15	0.13
MgO	8.1	9.4	8.0	8.2	8.2	8.5
CaO	12.1	13.9	12.2	12.4	14.1	14.3
Na_2O	2.2	2.3	2.3	2.2	2.4	2.3
K_2O	0.20	0.46	0.16	0.18	0.60	0.70
P_2O_5	0.14	0.19	0.12	0.13	0.27	0.23
L.O.I.		0.25	-0.63	-0.51	0.97	0.07
Sum	99.9	101.0	100.7	101.0	101.5	102.0
La	12.45	12.45	5.74	5.74	16.59	15.58
Ce	24.49	24.49	12.32	12.32	31.36	29.74
Pr	2.94	2.94	1.71	1.71	3.65	3.49
Nd	12.35	12.35	8.04	8.04	14.99	14.15
Sm	2.75	2.75	2.39	2.39	3.19	3.11
Eu	0.98	0.98	0.89	0.89	1.11	1.07
Gd	3.19	3.19	3.27	3.27	3.70	3.55
Tb	0.50	0.50	0.58	0.58	0.58	0.55
Dy	3.07	3.07	3.88	3.88	3.56	3.41
Ho	0.63	0.63	0.85	0.85	0.75	0.72
Er	1.74	1.74	2.39	2.39	2.08	2.00
Yb	1.62	1.62	2.34	2.34	1.97	1.91
Lu	0.25	0.25	0.36	0.36	0.30	0.29
Hf	1.9	1.87	1.62	1.62	2.05	1.84
$^{87}Sr/^{86}Sr$	0.702945	0.703118[b]	0.702957[b]	0.702933[c]	0.703109[b]	0.703049[c]
εNd	8.97	7.04	9.15	9.12	7.18	7.28
$^{206}Pb/^{204}Pb$	18.822	19.337	18.886	18.94	19.159	19.219
$^{207}Pb/^{204}Pb$	15.538	15.592	15.544	15.546	15.579	15.582
$^{208}Pb/^{204}Pb$	38.421	38.898	38.511	38.547	38.773	38.801
εHf	21.38	-	21.65	20.69	14.36	14.76

516 Table 1

Sample	B09-ROC14	B09-ROC15	B09-ROC20	B09-ROC21	B09-ROC22	B09-ROC23
Long. (°)	-32.276	-32.275	-32.280	-32.280	-32.280	-32.278
Lat. (°)	37.300	37.301	37.291	37.291	37.291	37.290
Type	E-MORB	E-MORB	T-MORB	T-MORB	T-MORB	T-MORB
SiO_2	-	48.7	51.6	51.8	51.7	51.6
TiO_2	-	1.01	1.06	1.06	1.05	1.05
Al_2O_3	-	17.9	14.3	15.0	15.0	15.1
FeO	-	6.7	10.3	10.0	9.9	9.5
MnO	-	0.14	0.19	0.19	0.18	0.18
MgO	-	8.7	8.2	8.1	8.1	8.2
CaO	-	14.5	12.3	12.3	12.2	12.5
Na_2O	-	2.2	2.3	2.3	2.3	2.2
K_2O	-	0.41	0.16	0.16	0.16	0.18
P_2O_5	-	0.18	0.13	0.13	0.12	0.13
L.O.I.	-	0.50	-0.78	-0.77	-0.77	-0.68
Sum	-	101.5	100.8	101.3	101.1	101.0
La	14.03	14.03	4.98	4.98	5.01	5.54
Ce	26.41	26.41	11.25	11.26	11.26	12.15
Pr	3.17	3.17	1.59	1.58	1.59	1.68
Nd	12.85	12.85	7.55	7.57	7.65	7.92
Sm	2.85	2.85	2.34	2.34	2.34	2.37
Eu	1.00	1.00	0.88	0.88	0.88	0.89
Gd	3.29	3.29	3.25	3.26	3.27	3.25
Tb	0.53	0.53	0.59	0.59	0.59	0.58
Dy	3.26	3.26	3.96	3.95	3.93	3.84
Ho	0.68	0.68	0.87	0.87	0.87	0.84
Er	1.90	1.90	2.46	2.47	2.45	2.37
Yb	1.83	1.83	2.45	2.46	2.45	2.34
Lu	0.28	0.28	0.38	0.38	0.38	0.36
Hf	1.69	1.69	1.59	1.59	1.58	1.61
$^{87}Sr/^{86}Sr$	-	0.70304[c]	0.702915[c]	0.702926[c]	0.702921[c]	0.702962[c]
εNd	6.10	7.00	9.25	9.40	9.21	9.15
$^{206}Pb/^{204}Pb$	19.355	-	18.888	18.884	18.89	18.932
$^{207}Pb/^{204}Pb$	15.591	-	15.543	15.545	15.544	15.547
$^{208}Pb/^{204}Pb$	38.93	-	38.507	38.513	38.511	38.542
εHf	14.32	14.98	21.97	22.12	21.76	-

517

518

519 Table 1

Sample	B09-ROC24	GRA N05-1	GRA N06-1	GRA N10-2	GRA N10-3	GRA N12-1
Long. (°)	-32.278	-32.220	-32.275	-32.237	-32.257	-32.235
Lat. (°)	37.290	37.285	37.291	37.280	37.285	37.280
Type	T-MORB	E-MORB	E-MORB	T-MORB	E-MORB	E-MORB
SiO_2	52.1	50.4	48.1	51.7	51.0	50.3
TiO_2	1.06	1.1	1.12	1.09	0.97	1.01
Al_2O_3	15.2	18.7	17.5	15.0	16.6	16.2
FeO	9.6	5.9	6.8	9.4	7.5	7.8
MnO	0.18	0.1	0.14	0.17	0.14	0.16
MgO	8.2	6.8	8.2	8.0	8.3	8.8
CaO	12.6	14.4	15.1	12.4	13.4	13.3
Na_2O	2.3	2.4	2.0	2.2	2.1	2.1
K_2O	0.18	0.3	0.46	0.18	0.41	0.30
P_2O_5	0.13	0.2	0.24	0.14	0.18	0.20
L.O.I.	-0.53	1.2	1.01	-0.26	0.21	0.53
Sum	102.1	102.1	101.5	101.2	101.6	101.5
La	5.60	8.51	14.01	6.08	11.65	8.68
Ce	12.36	16.93	27.49	13.41	22.36	17.54
Pr	1.70	2.19	3.36	1.83	2.68	2.22
Nd	8.03	9.69	13.90	8.39	11.08	9.63
Sm	2.40	2.50	3.15	2.45	2.58	2.38
Eu	0.90	1.02	1.12	0.92	0.92	0.91
Gd	3.27	3.16	3.57	3.29	3.13	2.96
Tb	0.59	0.53	0.57	0.58	0.51	0.50
Dy	3.87	3.38	3.50	3.78	3.23	3.15
Ho	0.85	0.72	0.73	0.82	0.69	0.67
Er	2.38	1.98	2.02	2.32	1.93	1.88
Yb	2.36	1.91	1.92	2.27	1.86	1.85
Lu	0.37	0.30	0.29	0.35	0.29	0.29
Hf	1.62	2.01	2.09	1.66	1.66	1.71
$^{87}Sr/^{86}Sr$	0.702981[b]	-	-	-	-	0.702978[b]
εNd	8.97	7.85	-	-	8.07	8.39
$^{206}Pb/^{204}Pb$	18.944	-	19.229	19.013	19.238	19.003
$^{207}Pb/^{204}Pb$	15.548	-	15.59	15.56	15.583	15.56
$^{208}Pb/^{204}Pb$	38.557	-	38.833	38.624	38.807	38.62
εHf	21.04	17.84	14.33	19.89	17.46	20.05

520

521
522

References

Agranier, A. et al., 2005. The spectra of isotopic heterogeneities along the mid-Atlantic Ridge. Earth and Planetary Science Letters, 238(1-2): 96-109.

Allègre, C.J., Hamelin, B., Dupré, B., 1984. Statistical analysis of isotopic ratios in MORB: the mantle blob cluster model and the convective regime of the mantle. Earth and Planetary Science Letters, 71: 71-84.

Andres, M., Blichert-Toft, J., Schilling, J.-G., 2004. Nature of the depleted upper mantle beneath the Atlantic: evidence from Hf isotopes in normal mid-ocean ridge basalts from 79°N to 55°S. Earth and Planetary Science Letters, 225(1-2): 89-103.

Andres, M., Blichert Toft, J., Schilling, J.G., 2002. Hafnium isotopes in bassalts from the southern Mid-Atlantic Ridge from 40°S to 55°S: Discovery and Shona plume-ridge interactions and the role of recycled sediments. G3, 3(10): 1-25.

Asimow, P.D., Dixon, J.E., Langmuir, C.H., 2004. A hydrous melting and fractionation model for mid-ocean ridge basalts: Application to the Mid-Atlantic Ridge near the Azores. Geochem. Geophys. Geosyst., 5(1): Q01E16.

Beier, C., Stracke, A., Haase, K.M., 2007. The peculiar geochemical signatures of São Miguel (Azores) lavas: Metasomatised or recycled mantle sources? Earth and Planetary Science Letters, 259(1-2): 186-199.

Blichert-Toft, J. et al., 2005. Geochemical segmentation of the Mid-Atlantic Ridge north of Iceland and ridge–hot spot interaction in the North Atlantic. Geochem. Geophys. Geosyst., 6(1): Q01E19.

Blichert-Toft, J., Albarede, F., 1997. The Lu-Hf isotope geochemistry of chondrites and the evolution of the mantle-crust system. Earth Planet. Sci. Lett., 148: 243-258.

Bonadiman, C., Beccaluva, L., Coltorti, M., Siena, F., 2005. Kimberlite-like Metasomatism and â€˜Garnet Signatureâ€™ in Spinel-peridotite Xenoliths from Sal, Cape Verde Archipelago: Relics of a Subcontinental Mantle Domain within the Atlantic Oceanic Lithosphere? Journal of Petrology, 46(12): 2465-2493.

Cannat, M. et al., 1999. Mid-Atlantic Ridgeâ€“Azores hotspot interactions: along-axis migration of a hotspot-derived event of enhanced magmatism 10 to 4 Ma ago. Earth and Planetary Science Letters, 173(3): 257-269.

Castillo, P., Batiza, R., 1989. Strontium, neodymium and lead isotope constraints on near-ridge seamount production beneath the South Atlantic. Nature, 342: 262-265.

Catanzaro, E.J., Murphy, T.J., Shields, W.R., Garner, E.L., 1968. Absolute Isotopic Abundance Ratios of Common, Equal-Atom, and Radiogenic Lead Isotopic Standards. Journal of Research of the National Bureau of Standards, 72A(3): 261-267.

Chauvel, C., BlichertToft, J., 2001. A hafnium isotope and trace element perspective on melting of the depleted mantle. Earth Planet Sci Lett, 190(3-4): 137-151.

Debaille, V. et al., 2006. Geochemical component relationships in MORB from the Mid-Atlantic Ridge, 22-35[degree sign]N. Earth and Planetary Science Letters, 241(3-4): 844-862.

Detrick, R.S., Needham, H.D., Renard, V., 1995. Gravity anomalies and crustal thickness variations along the Mid-Atlantic-Ridge between 33 degrees N and 40 degrees N. Journal of Geophysical Research - Solid Earth, 100(B3): 3767-3787.

Dosso, L., Bougault, H., Joron, J.L., 1993. Geochemical morphology of the North Mid-Atlantic Ridge, 10°-24°N: Trace element-isotopes complementarity. Earth and Planetary Science Letters, 120: 443-462.

Dosso, L. et al., 1999. The age and distribution of mantle heterogeneity along the Mid-Atlantic Ridge (31-41[degree sign]N). Earth and Planetary Science Letters, 170(3): 269-286.

Dosso, L., Hanan, B.B., Bougault, H., Schilling, J.G., Joron, J.L., 1991. Sr-Nd-Pb Geochemical Morphology Between 10-Degrees-N and 17-Degrees-N on the Mid-Atlantic Ridge - A New MORB Isotope Signature. Earth and Planetary Science Letters, 106(1-4): 29-43.

Douglass, J., Schilling, J.G., Fontignie, D., 1999. Plume-ridge interactions of the Discovery and Shona mantle plumes with the southern mid-Atlantic ridge (40 degrees-55 degrees S). J Geophys Res Solid Earth, 104(B2): 2941-2962.

Dupré, B., Allègre, C.J., 1983. Pb-Sr isotope variation in Indian Ocean basalts and mixing phenomena. Nature, 303: 142-146.

Elliott, T., Blichert-Toft, J., Heumann, A., Koetsier, G., Forjaz, V., 2007. The origin of enriched mantle beneath SÃ£o Miguel, Azores. Geochimica et Cosmochimica Acta, 71(1): 219-240.

Escartín, J., Cannat, M., Pouliquen, G., Rabain, A., Lin, J., 2001. Crustal thickness of V-shaped ridges south of the Azores: Interaction of the Mid-Atlantic Ridge (36°–39°N) and the Azores hot spot. J. Geophys. Res., 106(B10): 21719-21735.

Ferreira, P.L., 2006. Melt supply and magmatic evolution at a large central MOR volcano located in the Lucky Strike segment, 37°N on the Mid-Atlantic Ridge, Azores region, University of Southampton, 387 pp.

Fontignie, D., Schilling, J.G., 1996. Mantle heterogeneities beneath the South Atlantic: A Nd-Sr-Pb isotope study along the Mid-Atlantic Ridge (3 degrees S-46 degrees S). Earth and Planetary Science Letters, 142(1-2): 209-221.

Frey, F.A., Walker, N., Stakes, D., Hart, S.R., Nielsen, R., 1993. Geochemical Characteristics of Basaltic Glasses from the Amar and Famous Axial Valleys, Mid-Atlantic Ridge (36-Degrees-37-Degrees-N) - Petrogenetic Implications. Earth Planet Sci Lett, 115(1-4): 117-136.

Gale, A., Escrig, S., Gier, E.J., Langmuir, C.H., Goldstein, S.L., 2011. Enriched Basalts at Segment Centers: The Lucky Strike (37º 17' N) and Menez Gwen (37º 50' N) Segments of the Mid-Atlantic Ridge. Geochemistry, Geophysics, Geosystems, 12(6): Q06016.

Gente, P., Dyment, J., Maia, M., Goslin, J., 2003. Interaction between the Mid-Atlantic Ridge and the Azores hot spot during the last 85 Myr: Emplacement and rifting of the hot spot-derived plateaus. Geochem. Geophys. Geosyst., 4(10): 8514.

Gràcia, E., Bideau, D., Hekinian, R., Lagabrielle, Y., Parson, L.M., 1997. Along-axis magmatic oscillations and exposure of ultramafic rocks in a second-order segment of the Mid-Atlantic Ridge (33°43'N to 34°07'N). Geology, 25(12): 1059-1062.

Graham, D.W., Blichert-Toft, J., Russo, C.J., Rubin, K.H., Albarede, F., 2006. Cryptic striations in the upper mantle revealed by hafnium isotopes in southeast Indian ridge basalts. Nature, 440(7081): 199-202.

Griffin, W.L., Oâ€™Reilly, S.Y., Afonso, J.C., Begg, G.C., 2009. The Composition and Evolution of Lithospheric Mantle: a Re-evaluation and its Tectonic Implications. Journal of Petrology, 50(7): 1185-1204.

Hamelin, B., Dupré, B., Allègre, C.J., 1984. Lead-strontium isotopic variations along the East Pacific Rise and the Mid-Atlantic Ridge: a comparative study. Earth and Planetary Science Letters, 67: 340-350.

Hamelin, C. et al., 2011. Geochemical portray of the Pacific Ridge: New isotopic data and statistical techniques. Earth and Planetary Science Letters, 302(1-2): 154-162.

615 **Hanan, B.B., Blichert-Toft, J., Pyle, D.G., Christie, D.M., 2004. Contrasting origins of the**
616 **upper mantle revealed by hafnium and lead isotopes from the Southeast Indian Ridge.**
617 **Nature, 432: 91-94.**
618 **Hanan, B.B., Graham, D.W., 1996. Lead and Helium isotope evidence from oceanic basalts for**
619 **a common deep source of mantle plumes. Science, 272: 991-995.**
620 **Hanan, B.B., Kingsley, R.H., Schilling, J.-G., 1986. Pb isotope evidence in the South Atlantic for**
621 **migrating ridge-hotspot interactions. Nature, 322: 137-144.**
622 **Hart, S., Hauri, E.H., Oschmann, L.A., Whitehead, J.A., 1992. Mantle plumes and**
623 **entrainment: isotopic evidence. Science, 256: 517-520.**
624 **Harvey, J. et al., 2006. Ancient melt extraction from the oceanic upper mantle revealed by Re-**
625 **Os isotopes in abyssal peridotites from the Mid-Atlantic ridge. Earth and Planetary**
626 **Science Letters, 244(3-4): 606-621.**
627 **Hofmann, A.W., Heinrich, D.H., Karl, K.T., 2003. Sampling Mantle Heterogeneity through**
628 **Oceanic Basalts: Isotopes and Trace Elements, Treatise on Geochemistry. Pergamon,**
629 **Oxford, pp. 1-44.**
630 **Ito, E., White, W.M., Göpel, C., 1987. The O, Sr, Nd and Pb isotope geochemistry of MORB.**
631 **Chemical Geology, 62: 157-176.**
632 **Janney, P.E., Le Roex, A.P., Carlson, R.W., 2005. Hafnium Isotope and Trace Element**
633 **Constraints on the Nature of Mantle Heterogeneity beneath the Central Southwest**
634 **Indian Ridge (13Â°E to 47Â°E). Journal of Petrology, 46(12): 2427-2464.**
635 **Langmuir, C. et al., 1997. Hydrothermal vents near a mantle hot spot: The Lucky Strike vent**
636 **field at 37 degrees N on the Mid-Atlantic Ridge. Earth and Planetary Science Letters,**
637 **148(1-2): 69-91.**
638 **Liu, C.-Z. et al., 2008. Ancient, highly heterogeneous mantle beneath Gakkel ridge, Arctic**
639 **Ocean. Nature, 452: 311-316.**
640 **Machado, N., Ludden, J.N., Brooks, C., Thompson, G., 1982. Fine scale isotopic heterogeneity**
641 **in the sub-Atlantic mantle. Nature, 295: 226-228.**
642 **Madureira, P., Mata, J.o., Mattielli, N., Queiroz, G., Silva, P., 2011. Mantle source**
643 **heterogeneity, magma generation and magmatic evolution at Terceira Island (Azores**
644 **archipelago): Constraints from elemental and isotopic (Sr, Nd, Hf, and Pb) data. Lithos,**
645 **126(3â€“4): 402-418.**
646 **Manhes, G., Minster, J.F., Allègre, C.J., 1978. Comparative uranium-thorium-lead and**
647 **rubidium-strontium study of the Saint Sèverin amphoterite: consequences for early**
648 **solar system chronology. Earth and Planetary Science Letters, 39(1): 14-24.**
649 **Meyzen, C.M. et al., 2007. Isotopic portrayal of the Earth/'s upper mantle flow field. Nature,**
650 **447(7148): 1069-1074.**
651 **Miranda, J.M., Luis, J.F., Lourenço, N., Santos, F.M., 2005. Identification of the magnetization**
652 **low of the Lucky Strike hydrothermal vent using surface magnetic data. J. Geophys.**
653 **Res., 110(B4): B04103.**
654 **Moreira, M., Doucelance, R.g., Kurz, M.D., DuprÃ©, B., AllÃ¨gre, C.J., 1999. Helium and lead**
655 **isotope geochemistry of the Azores Archipelago. Earth and Planetary Science Letters,**
656 **169(1â€“2): 189-205.**
657 **Moreira, M. et al., 2011. Rare gas systematics on Lucky Strike basalts (37°N, North Atlantic):**
658 **Evidence for efficient homogenization in a long-lived magma chamber system? Geophys.**
659 **Res. Lett., 38(8): L08304.**
660 **Morgan, J.P., Morgan, W.J., 1999. Two-stage melting and the geochemical evolution of the**
661 **mantle: a recipe for mantle plum-pudding. Earth Planet Sci Lett, 170(3): 215-239.**

Nowell, G.M. et al., 1998. High precision Hf isotope measurements of MORB and OIB by thermal ionisation mass spectrometry: insights into the depleted mantle. Chemical Geology, 149(3-4): 211-233.

Patchett, P.J., Tatsumoto, M., 1980. Hafnium isotope variations in oceanic basalts. Geophysical Research Letters, 7: 1077-1080.

Paulick, H., Münker, C., Schuth, S., 2010. The influence of small-scale mantle heterogeneities on Mid-Ocean Ridge volcanism: Evidence from the southern Mid-Atlantic Ridge (7°30'S to 11°30'S) and Ascension Island. Earth and Planetary Science Letters, 296(3-4): 299-310.

Salters, V.J.M., 1996. The generation of mid-ocean ridge basalts from the Hf and Nd isotope perspective. Earth and Planetary Science Letters, 141(1-4): 109-123.

Salters, V.J.M., Dick, H.J.B., 2002. Mineralogy of the mid-ocean-ridge basalt source from neodymium isotopic composition of abyssal peridotites. nature, 418(6893): 68-72.

Salters, V.J.M., Hart, S.R., 1989. The hafnium paradox and the role of garnet in the source of mid-ocean ridge basalts. Nature, 342: 420-422.

Salters, V.J.M., Mallick, S., Hart, S.R., Langmuir, C.E., Stracke, A., 2011. Domains of depleted mantle: New evidence from hafnium and neodymium isotopes. Geochem. Geophys. Geosyst., 12(8): Q08001.

Salters, V.J.M., Stracke, A., 2004. Composition of the depleted mantle. Geochem. Geophys. Geosyst., 5(5): Q05B07.

Salters, V.J.M., White, W.M., 1998. Hf isotope constraints on mantle evolution. Chemical Geology, 145: 447-460.

Salters, V.J.M., Zindler, A., 1995. Extreme Hf-176/Hf-177 in the sub-oceanic mantle. Earth and Planetary Science Letters, 129(1-4): 13-30.

Schiano, P., Birck, J.L., Allegre, C.J., 1997. Osmium-strontium-neodymium-lead isotopic covariations in mid-ocean ridge basalt glasses and the heterogeneity of the upper mantle. Earth and Planetary Science Letters, 150(3-4): 363-379.

Schilling, J.G., 1975. Azores mantle blob: rare earth evidence. Earth and Planetary Science Letters, 25: 103-115.

Schilling, J.G., Hanan, B.B., McCully, B., Kingsley, R.H., Fontignie, D., 1994. Influence of the Sierra Leone mantle plume on the equatorial Mid-Atlantic Ridge: A Nd-Sr-Pb isotopic study. J. Geophys. Res., 99(B6): 12005-12028.

Seyler, M., Cannat, M., Mével, C., 2003. Evidence for major-element heterogeneity in the mantle source of abyssal peridotites from the Southwest Indian Ridge (52° to 68°E). Geochem. Geophys. Geosyst., 4(2): 9101.

Shirey, S.B., Bender, J.F., Langmuir, C.H., 1987. Three-component isotopic heterogeneity near the Oceanographer transform Mid-Atlantic Ridge. Nature, 325: 217-223.

Simon, N.S.C., Carlson, R.W., Pearson, D.G., Davies, G.R., 2007. The Origin and Evolution of the Kaapvaal Cratonic Lithospheric Mantle. Journal of Petrology, 48(3): 589-625.

Singh, S.C. et al., 2006. Discovery of a magma chamber and faults beneath a Mid-Atlantic Ridge hydrothermal field. nature, 442(7106): 1029-1032.

Stracke, A., Bizimis, M., Salters, V.J.M., 2005. Recycling oceanic crust: Quantitative constraints. G cubed, 4(3): 1-33.

Stracke, A. et al., 2011. Abyssal peridotite Hf isotopes identify extreme mantle depletion. Earth and Planetary Science Letters, 308(3-4): 359-368.

Van Orman, J., Grove, T., Shimizu, N., Layne, G., 2002. Rare earth element diffusion in a natural pyrope single crystal at 2.8 GPa. Contributions to Mineralogy and Petrology, 142(4): 416-424.

Vlastelic, I. et al., 1999. Large-scale chemical and thermal division of the Pacific mantle. Nature, 399: 345-350.

Widom, E., Carlson, R.W., Gill, J.B., Schmincke, H.U., 1997. Thâ€“Srâ€“Ndâ€“Pb isotope and trace element evidence for the origin of the SÃ£o Miguel, Azores, enriched mantle source. Chemical Geology, 140(1â€“2): 49-68.

Yu, D., Fontignie, D., Schilling, J.-G., 1997. Mantle plume-ridge interactions in the Central North Atlantic: a Nd isotope study of mid-Atlantic Ridge basalts from 30°N to 50°N. Earth and Planetary Science Letters, 146: 259-272.

Zindler, A., Hart, S., 1986. Chemical geodynamics. Annual Review of Earth and Planetary Sciences, 14: 493-571.

Figure 1

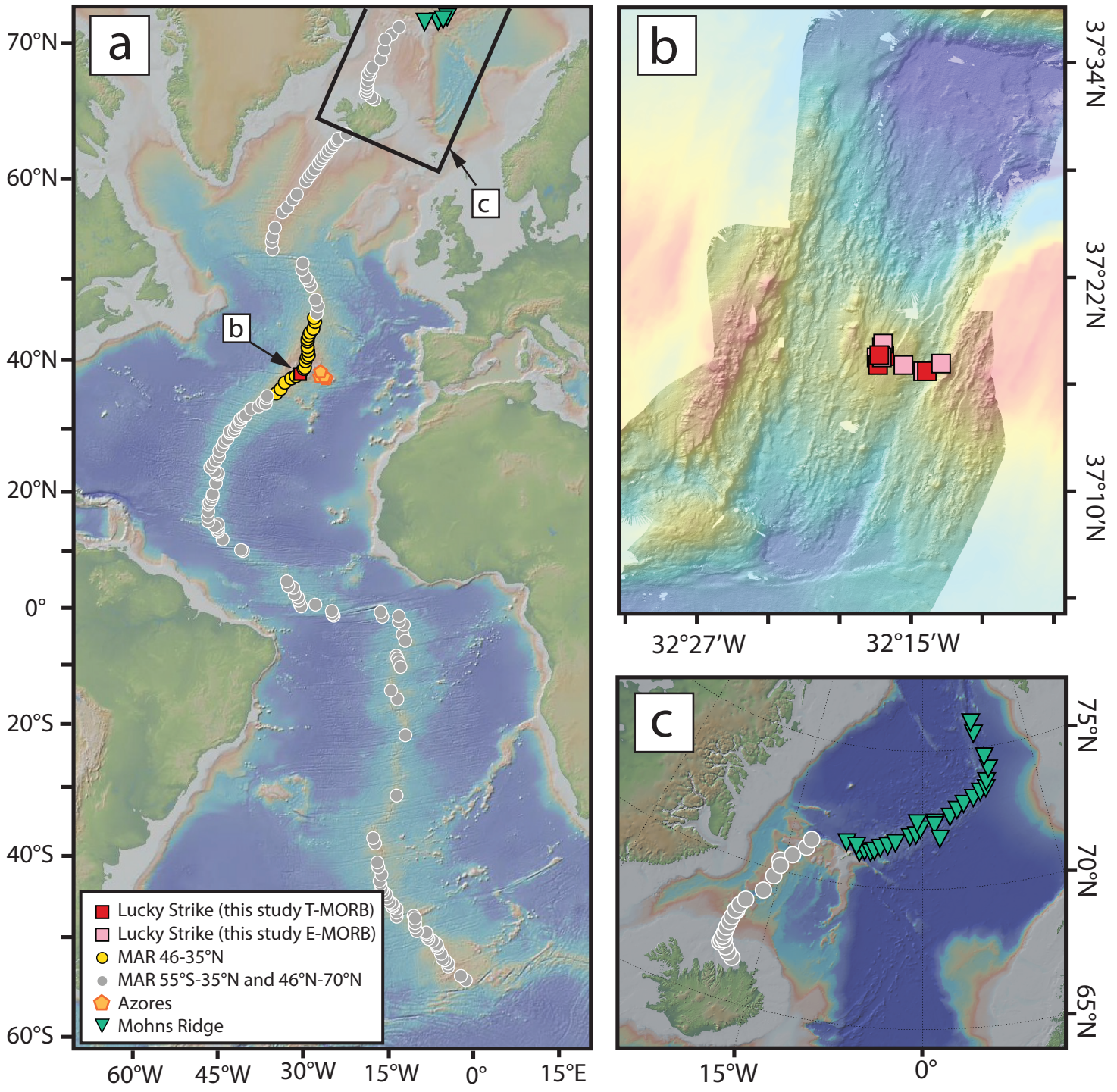
a
b
c
70°N
60°N
40°N
20°N
0°
20°S
40°S
60°S
60°W
45°W
30°W
15°W
0°
15°E
Lucky Strike (this study T-MORB)
Lucky Strike (this study E-MORB)
MAR 46-35°N
MAR 55°S-35°N and 46°N-70°N
Azores
Mohns Ridge
37°34'N
37°22'N
37°10'N
32°27'W
32°15'W
75°N
70°N
65°N
15°W
0°

Figure 2

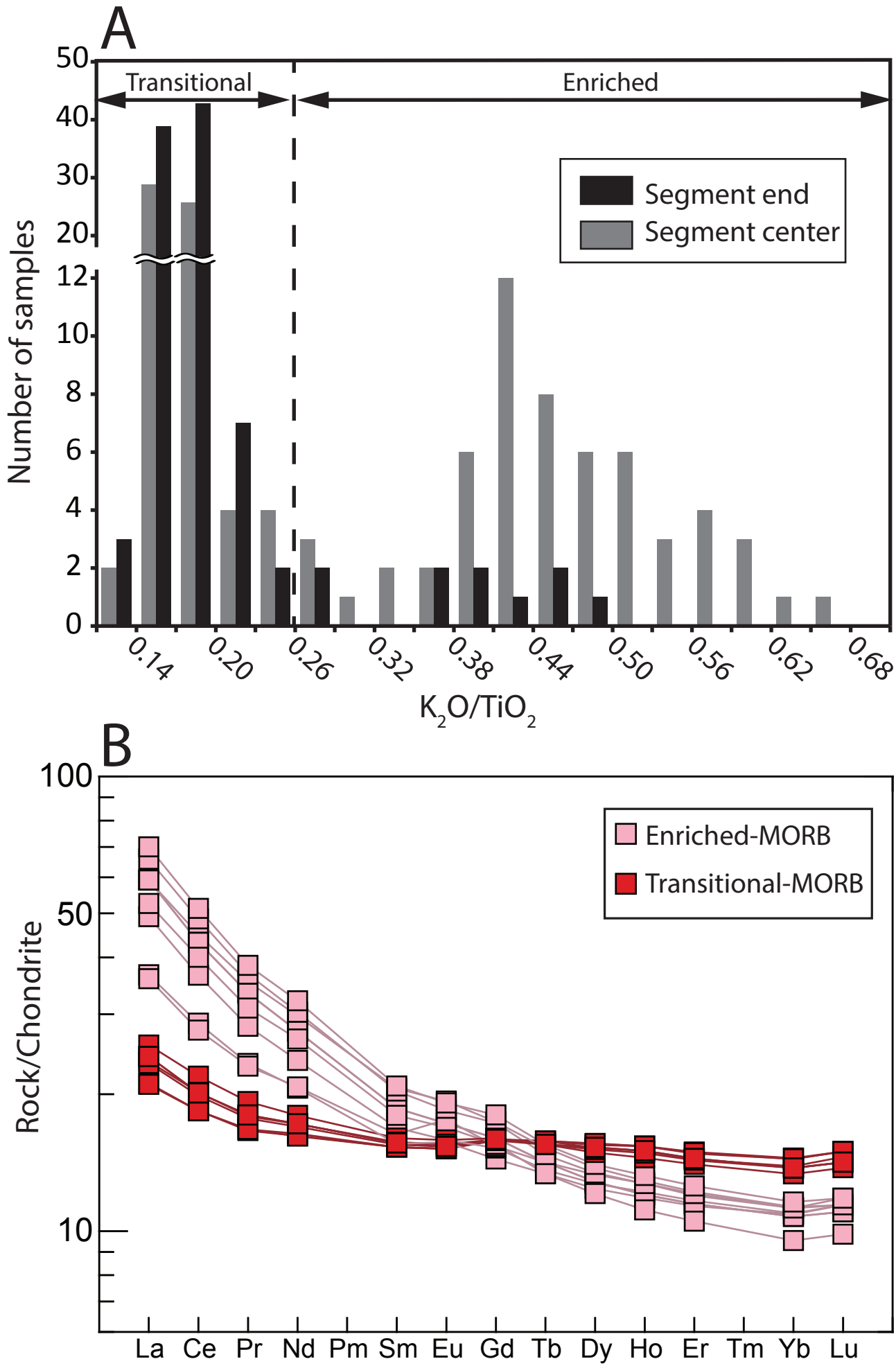
A
Transitional
Enriched
Segment end
Segment center
Number of samples
50
40
30
20
12
10
8
6
4
2
0
0.14
0.20
0.26
0.32
0.38
0.44
0.50
0.56
0.62
0.68
K2O/TiO2
B
Enriched-MORB
Transitional-MORB
Rock/Chondrite
100
50
10
La
Ce
Pr
Nd
Pm
Sm
Eu
Gd
Tb
Dy
Ho
Er
Tm
Yb
Lu

Figure 3

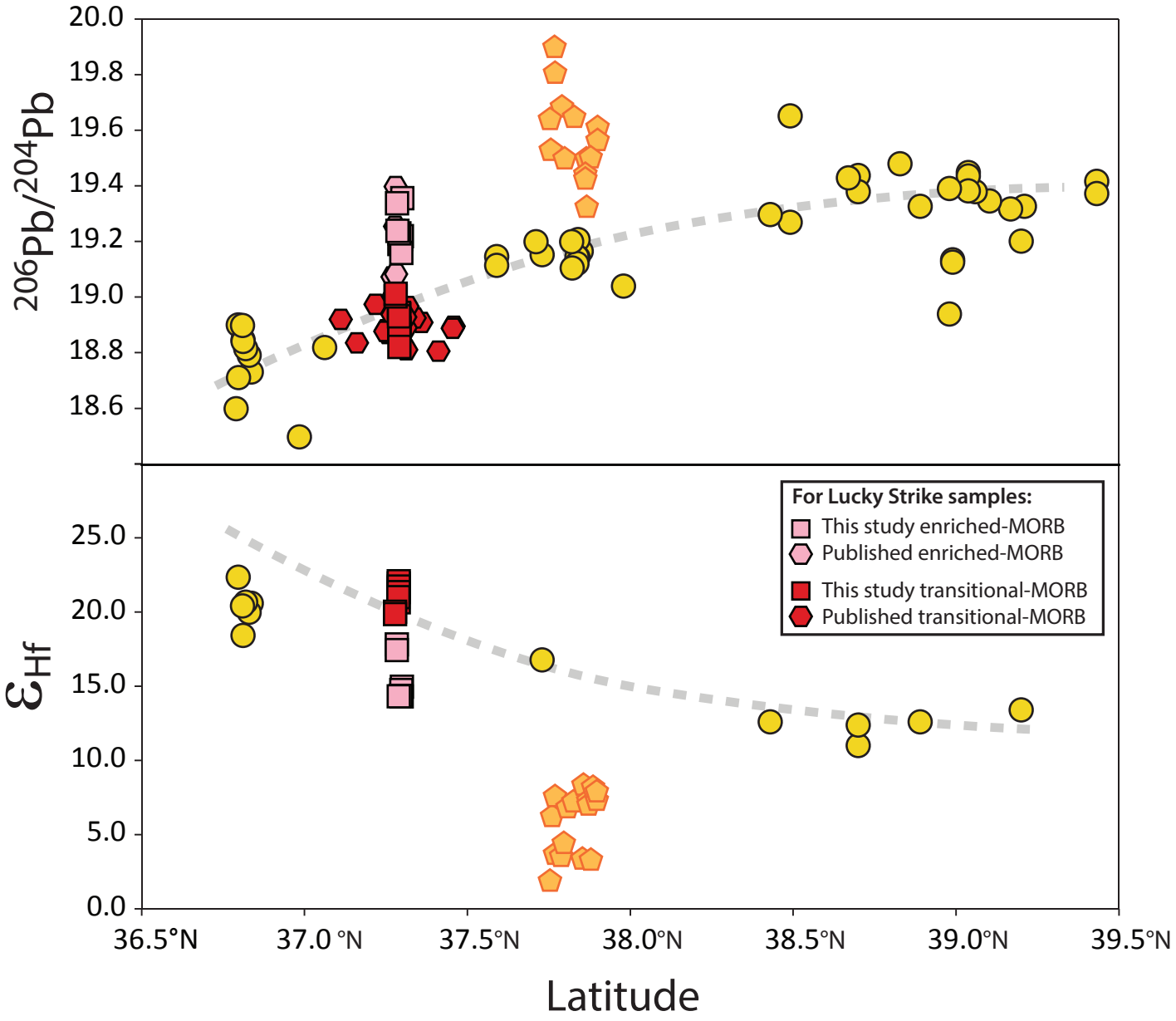
20.0
19.8
19.6
19.4
19.2
19.0
18.8
18.6
$^{206}Pb/^{204}Pb$
25.0
20.0
15.0
10.0
5.0
0.0
ε_{Hf}
For Lucky Strike samples:
This study enriched-MORB
Published enriched-MORB
This study transitional-MORB
Published transitional-MORB
36.5°N
37.0 °N
37.5°N
38.0°N
38.5°N
39.0°N
39.5°N
Latitude

Figure 4

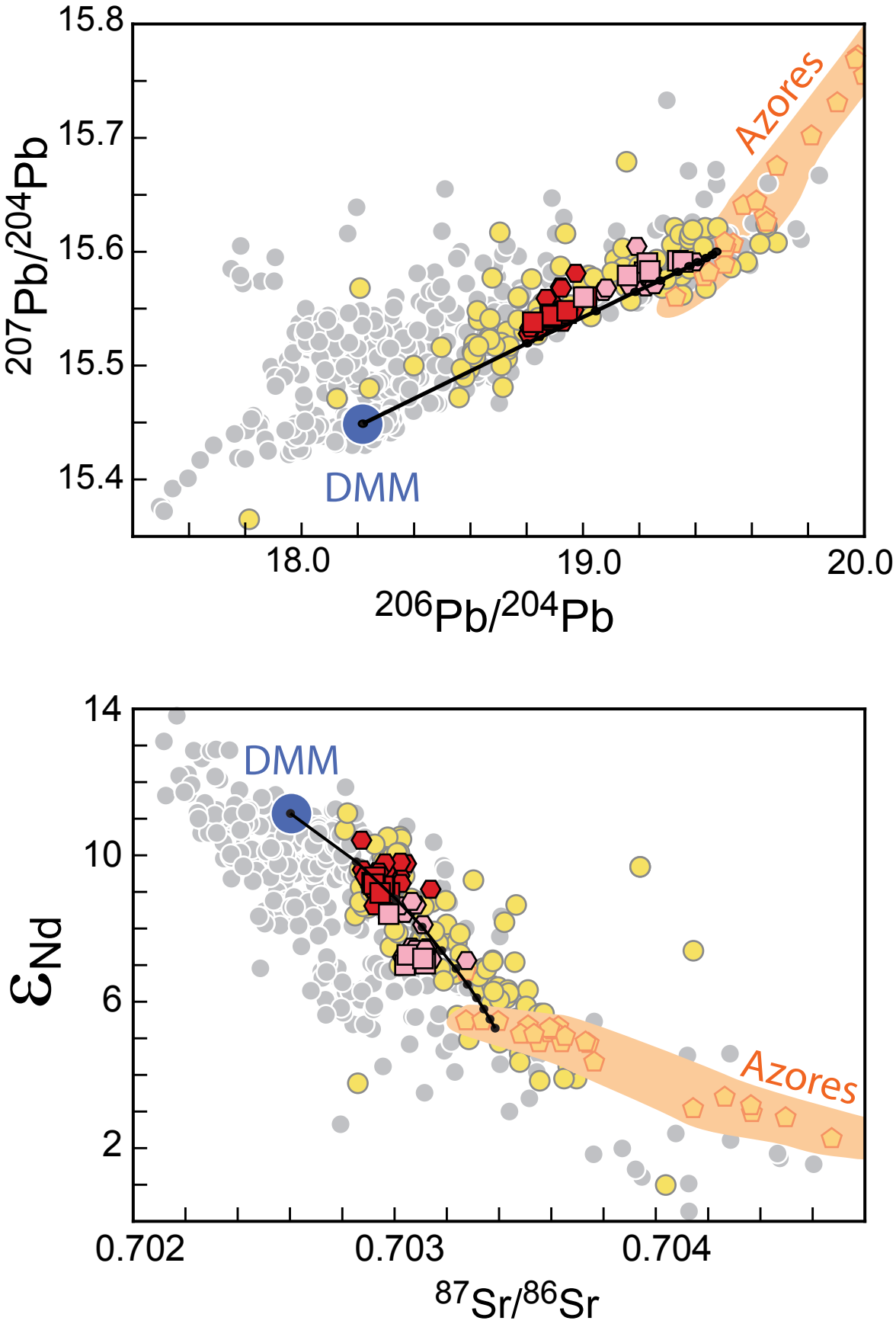
15.8
15.7
15.6
15.5
15.4
$^{207}Pb/^{204}Pb$
18.0
19.0
20.0
$^{206}Pb/^{204}Pb$
Azores
DMM
14
10
6
2
ε_{Nd}
0.702
0.703
0.704
$^{87}Sr/^{86}Sr$
DMM
Azores

Figure 5

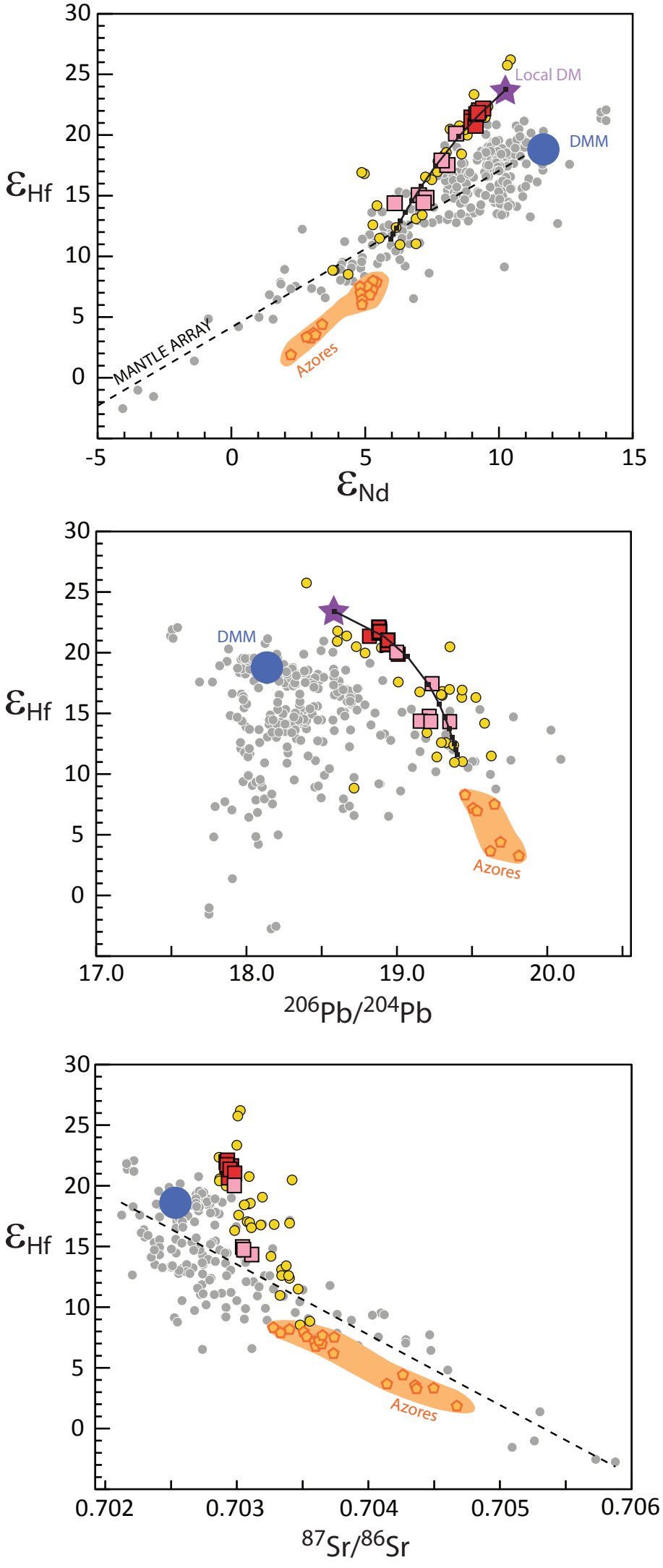
30
25
20
15
10
5
0
εHf
-5
0
5
10
15
εNd
Local DM
DMM
MANTLE ARRAY
Azores
17.0
18.0
19.0
20.0
206Pb/204Pb
0.702
0.703
0.704
0.705
0.706
87Sr/86Sr

Figure 6

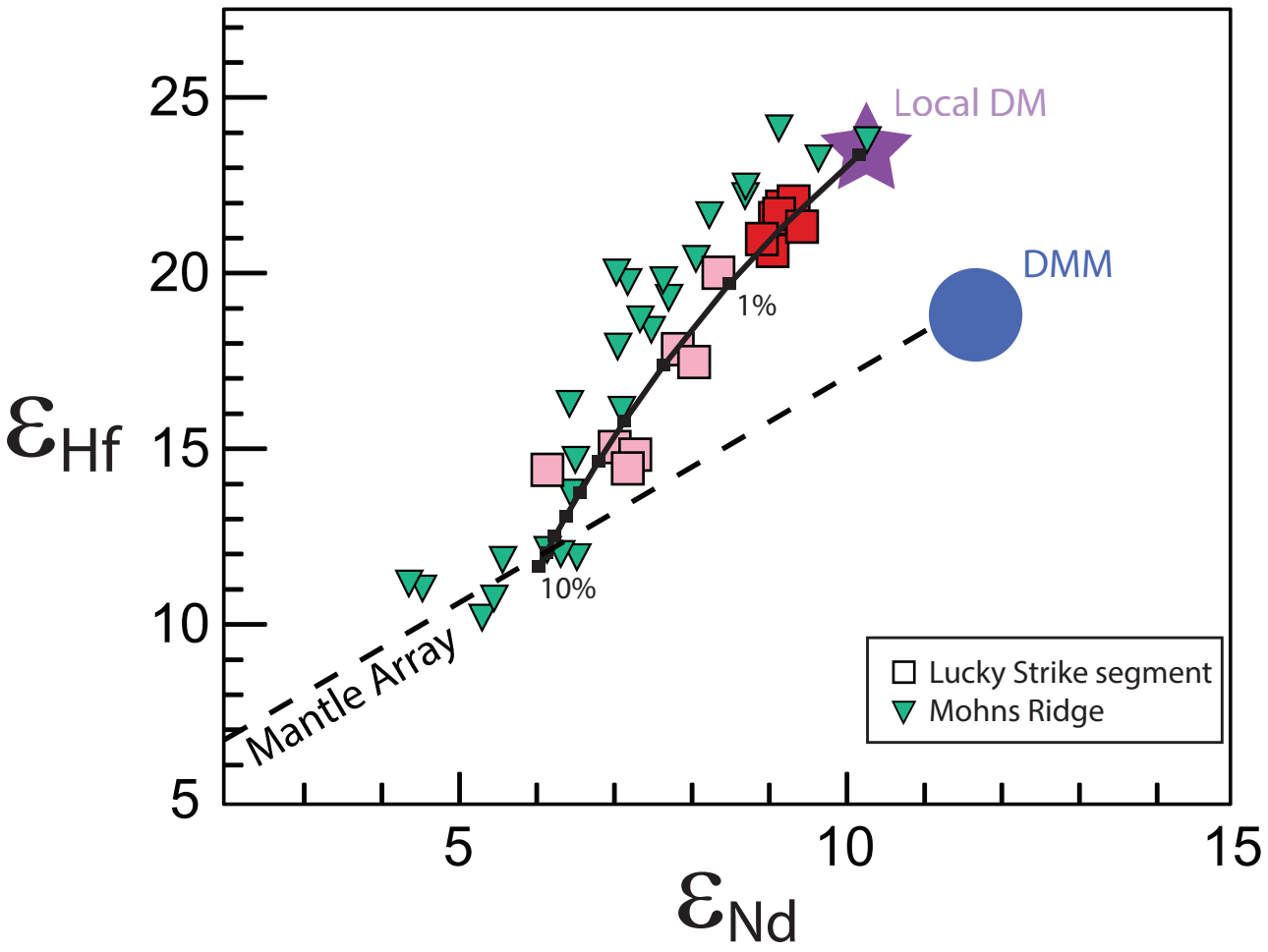
25
20
15
10
5
εHf
5
10
15
εNd
Local DM
DMM
1%
10%
Mantle Array
Lucky Strike segment
Mohns Ridge

Figure 7

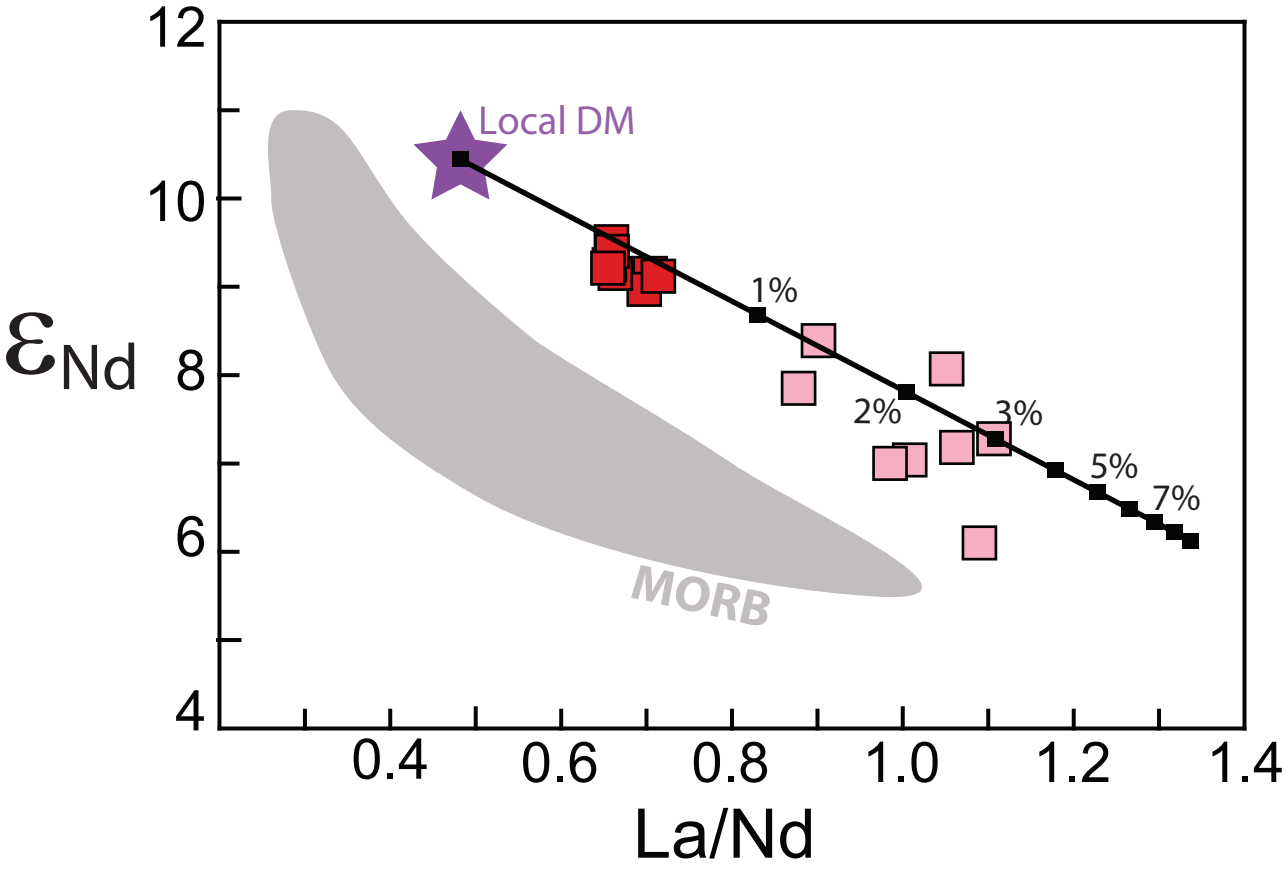
Local DM
1%
2%
3%
5%
7%
MORB
12
10
8
6
4
εNd
0.4
0.6
0.8
1.0
1.2
1.4
La/Nd

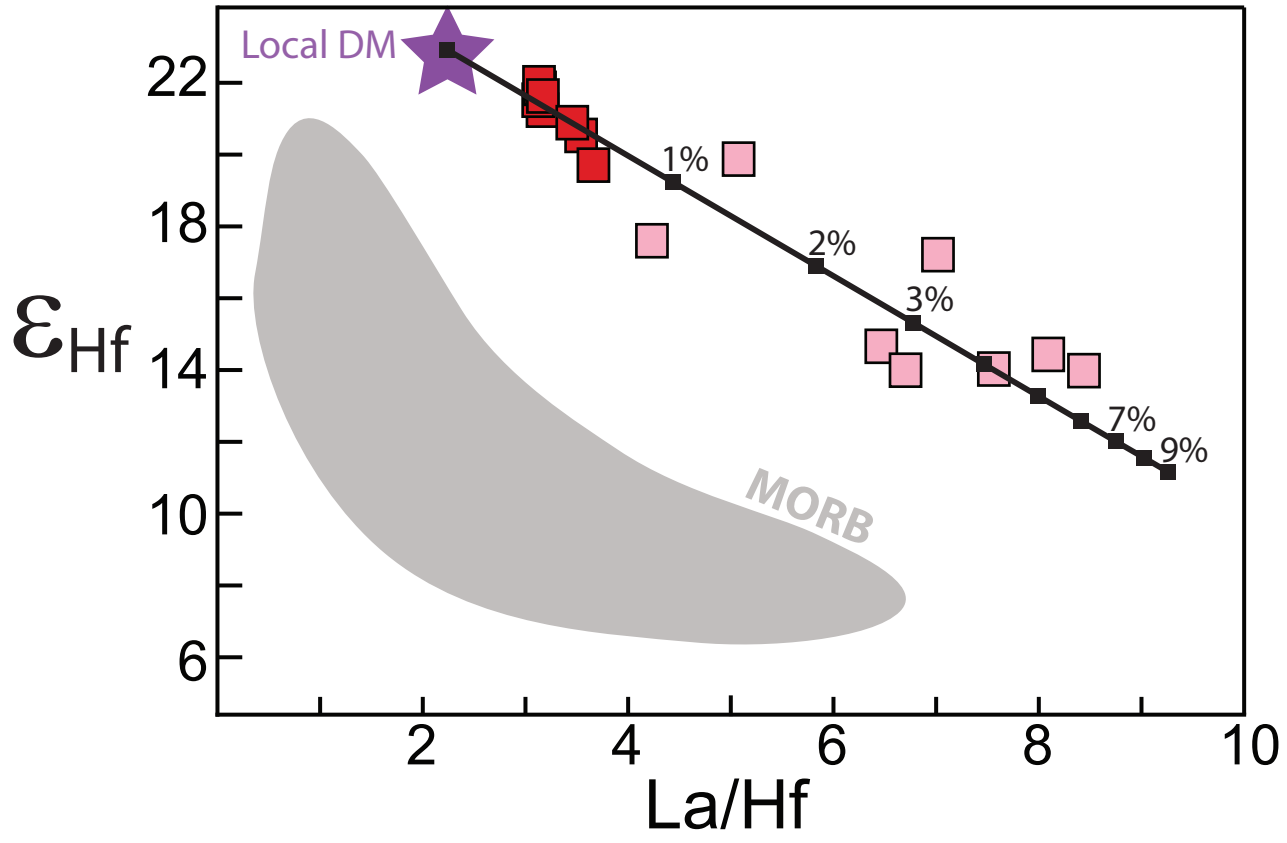
Local DM
1%
2%
3%
7%
9%
MORB
22
18
14
10
6
εHf
2
4
6
8
10
La/Hf

Figure 8

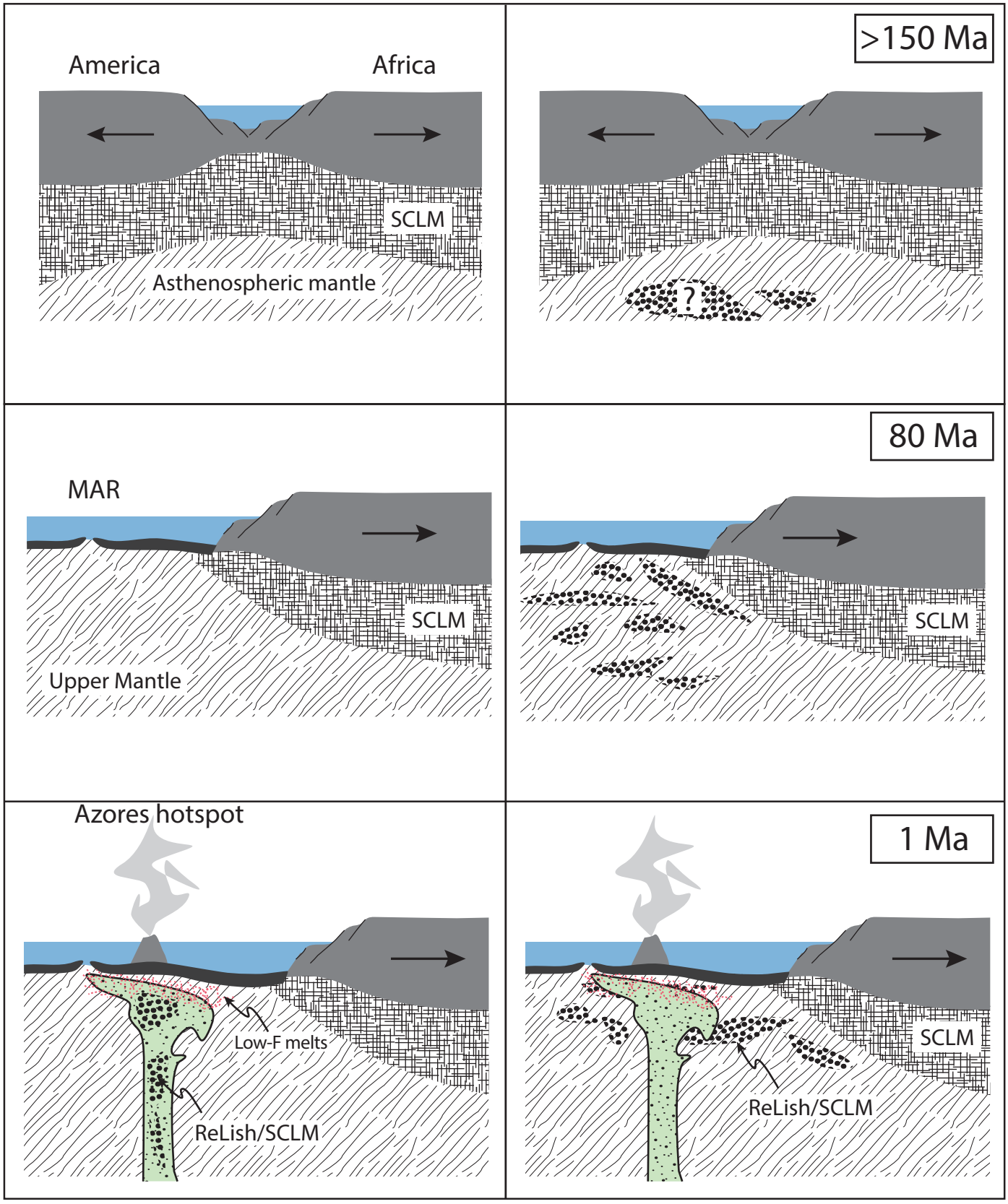

A) Atypical depleted component as a primary constituent of Azores Hotspot	B) Atypical depleted component as a part of the upper mantle